Paste 2023 – GW Wilson, NA Beier, DC Sego, AB Fourie & D Reid (eds)

doi:10.36487/ACG_repo/2355_11

Assessment of static liquefaction susceptibility of early age cemented paste backfills

T Belem *Université du Québec en Abitibi-Témiscamingue, Canada*

M Mbonimpa *Université du Québec en Abitibi-Témiscamingue, Canada*

J Oke *RockEng, Canada*

LP Gélinas *Agnico Eagle Mines Limited, Canada*

Abstract

The use of cemented paste backfills (CPB) for stope filling as a tailings management method becomes almost indispensable for flexible, selective and safe underground mining operations. For CPB to play the role of secondary ground support, it must develop a certain uniaxial compressive strength (UCS). The UCS value is almost linearly proportional to the binder content used. However, the cost of the binder represents 8 to 16% of the operating costs of mining with cemented backfill. That is the reason why mining companies seek to reduce the binder cost by reducing the amount of binder in the CPB mixtures. Unfortunately, a reduction in the binder content could cause a significant decrease in CPB strength, particularly at early ages. Such a CPB strength reduction, under undrained conditions, may cause liquefaction-induced failures at early ages due to seismic shaking or static loading. Static liquefaction can occur if the CPB show contractive behaviour during undrained loading and if there is a triggering mechanism present. The triggering mechanism can be due to a rapid rate of CPB raising (overloading), changes in porewater pressure or reduction in lateral confinement. The objective of this study is to experimentally assess the static liquefaction susceptibility of CPB containing low percentages of HS Portland cement (1.5, 1.75 and 2 wt%) at early ages (3 and 7 days). For each cement percentage and both curing times, isotropically consolidated undrained (CIU) triaxial compression tests were performed. Preliminary results are provided and the conditions for static liquefaction triggering are either null effective minor stress or when the pore pressure ratio (r_u) reaches or is close to unity ($r_u = \Delta u/\sigma'_3 = 1$). The results showed that only the CPB studied using 1.5 wt% cement reached the condition of initial static liquefaction temporarily (axial strain in the range 0.5–3.5%) before resisting against liquefaction development (dilative behaviour).

Keywords: *static liquefaction, cemented paste backfill (CPB), unconfined compressive strength (UCS), consolidated undrained triaxial, contractive behaviour*

1 Introduction

Mining operations create many jobs and generate considerable socio-economic benefits but they also generate a large amount of solid waste, such as mill tailings and waste rock, which need to be properly managed in mine waste disposal areas (i.e. tailings storage facilities and waste rock stockpiles). Inappropriate management of these solid wastes could result in instabilities that are hydrogeochemical (e.g. production of contaminated mine drainage) and/or geotechnical (failure of tailings storage facilities and their release into the environment) in nature (Aubertin et al. 2002). The mining industry has a duty to prevent and/or mitigate the impacts of its activities on the environment by implementing land conservation measures and by optimising its practices in a sustainable development context. In Canada, the mining industry is obliged to reduce its ecological footprint to a minimum through the Towards Sustainable Mining initiative advocated by the Mining Association of Canada. When mining underground, nearly half of the generated mill tailings can be returned underground as cemented paste backfill (CPB) with the addition of a binding agent, hence improving ground support and ore recovery (Benzaazoua et al. 2002, 2004; Potvin et al. 2004; Belem & Benzaazoua 2008).

CPB is a mixture of mill tailings, a binding agent (e.g. type GU, HE or HS Portland cement, or a blend of a Portland cement and one of the supplementary cementitious materials such as ground granulated blast furnace slag, type F fly ash or type C fly ash etc.) and mixing water. The purpose of a binder addition is to develop typical uniaxial compressive strength (UCS) values ranging from 150 kPa up to about 5 MPa, depending on the role that the CPB must play (e.g. confined block, self-supporting pillar, sill mat, working floor etc.).

The use of CPB for open stopes filling as a tailings management method becomes almost indispensable for flexible, selective and safe underground mining operations. However, underground mining with backfill must meet both transport (flowability) and stability (secondary ground support requirements) criteria once placed. Indeed, for the backfill to play its full role in relation to the mining method employed it must develop a targeted strength corresponding to a certain UCS or undrained shear strength value (Belem & Benzaazoua 2008). Meeting these criteria eliminates some of the operational risks such as blockage of the CPB distribution line or any failure of the CPB mass that could result in equipment damage and/or human injuries. Indeed, for various operational reasons, it frequently happens that the distribution line is blocked or that the UCS of the CPB does not reach its design requirement to guarantee ground stability (Belem & Benzaazoua 2008). This may be due to the physicochemical properties of the CPB mixture ingredients, the mineralogy of the mill tailings, the underdosing of the binding agent or excess water in the CPB mixture. In this context, the simplest solution could be to overdose the binding agent to improve the gain in compressive strength, because the UCS value is almost linearly proportional to the binder content used (Belem et al. 2000; Benzaazoua et al. 2002; Belem & Benzaazoua 2008).

CPB costs generally account for between 10 and 20% of the total operating expense of a mine and a hydraulic binder represents up to 75–80% of that cost (Grice 1998). This means that the price of the binder represents between 8 and 16% of the operating budget of mining with CPB. This is the main reason why mining companies are seeking to reduce the binder cost by reducing the amount of binder in the CPB mixtures. Unfortunately, a reduction in the amount of binder could lead to a substantial decrease in the mechanical properties of CPB, particularly at early ages (i.e. from 0 to 7 days of curing). Such a reduction in the mechanical properties of CPB may trigger, under undrained loading conditions, liquefaction-induced failures due to seismic shakings (cyclic softening or failure) caused by several sources including consecutive sequences of blasting, rockburst, seismic events, ground vibration, earthquake etc. (le Roux et al. 2004; Belem et al. 2013; Belem & Mbonimpa 2016).

Liquefaction is a term most often associated with seismic events. In common usage, liquefaction refers to a phenomenon wherein a shear resistance of a mass of saturated loose material decreases due to the build-up of porewater pressures during monotonic, cyclic or dynamic loading at constant volume (Poulos et al., 1985; Sladen et al. 1985). However, mine tailings impoundments have demonstrated more static liquefaction events than seismic induced events (Kramer & Seed 1988; Fourie et al. 2001; Davies et al. 2002). Static liquefaction or flow failure can be triggered in undrained conditions because of rapid static loading that triggers significant shear-induced pore pressure rise (Davies et al. 2002). It is assumed that factors which can contribute to the occurrence of static liquefaction of CPB are contractive behaviour of the fresh mixture, overloading (a rapid rate of raise of CPB), changes in pore pressures, virtually no water drainage or a reduction in lateral confinement (Aref 1988; Davies et al. 2002; le Roux et al. 2004). Dilative soils are not susceptible to liquefaction because their undrained shear strength is greater than their drained strength. Based on the concept of a steady state of deformation, only soils that tend to decrease in volume during shear, i.e. contractive soils, can suffer the necessary loss of shear resistance to result in liquefaction (Poulos et al. 1985).

The main objective of this study is to assess experimentally the static liquefaction susceptibility of CPB mixtures prepared with low mass proportions of cement (≤ 2%) using isotropically consolidated undrained (CIU) triaxial compression tests at early ages (≤ 7 days). More specifically, this study aims at investigating the mechanical behaviour of CPB mixtures under undrained conditions to evaluate under which circumstances (in terms of contractive or dilative) static liquefaction does or does not occur. The mining industry's tendency to seek to reduce the amount of binder added in the preparation of CPB can represent the potential risk of flowing of the backfill mass due to static liquefaction when a barricade is loaded during a continuous pouring operation. Indeed, the liquefaction resistance increases with increasing cement content (Aref 1988).

2 Methodology

2.1 Tailings sample physicochemical and mineralogical characterisations

A representative test sample from Canadian zinc mine Brunswick's (BWK) highly sulfide-rich and fine tailings was homogenised for various analyses to determinate the following parameters: gravimetric water content *w* (%) by oven-drying at 40°C until mass stabilisation, relative density of grains or specific gravity (D_R or G_s) using a Micromeritics Accupyc 1330 helium pycnometer, specific surface area (SSA) determined by nitrogen multi-point adsorption isotherms based on the Brunauer–Emmett–Teller (BET) adsorption theory using a Micromeritics Gemini III 2375 surface analyser, grain size distribution (GSD) using a Malvern Panalytical Mastersizer laser diffraction grain size analyser, chemical composition determined using an ICP-AES (PerkinElmer apparatus) after total acid digestion, and mineralogical composition by X-ray diffractograms (XRD) using a Bruker's apparatus (the semi-quantification of minerals is obtained by the Rietveld method with TOPAS software).

The tailings tested had an initial water content of *w* = 18.1% (corresponding to solids mass concentration $C_w = 100*M_{solids}/M_{total}$ = 84.7%), a BET specific surface area of 1.75 m^2/g and a relative density ($D_R = G_s$) of 4.03. Tables 1 and 2 present the physical properties, and the chemical and mineralogical compositions, of the BWK mine tailings, respectively. Figure 1 presents the GSD curves of the BWK mine tailings sample. The high value of G_s can be explained by the high sulfide content of about 60% (see Table 2).

Table 1 Physical properties of the BWK mine tailings

Parameter	Unit	Value
$C_U = D_{60}/D_{10}$	(-)	12.4
$C_C = D_{30}^2/(D_{60}*D_{10})$	(-)	1.6
$U = (D_{90}-D_{10})/D_{50}$	(-)	3.7
D_{10}	(µm)	1.7
D_{30}	(µm)	7.5
D_{50}	(µm)	15.5
D_{60}	(µm)	21.2
D_{80} (fines)	(µm)	39.5
D_{90}	(µm)	58.8
$P_{20\mu m}$ (ultra-fines)	(%)	57.9

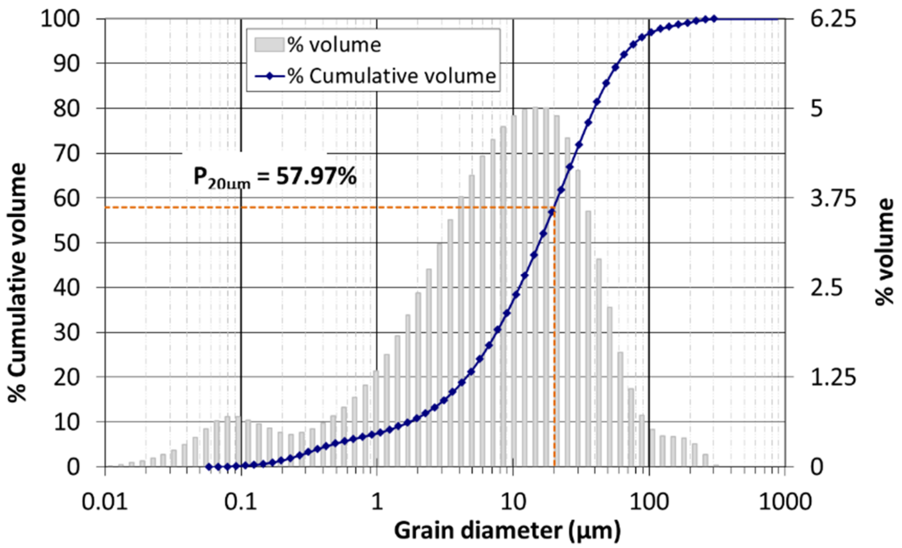

Figure 1 Grain size distribution curves of the BWK mine tailings

Table 2 Chemical composition and the mineralogical composition of the BWK mine tailings

Chemical composition		Mineralogical composition	
Element	**Amount in wt%**	**Mineral**	**Amount in wt%**
Al	0.751	Quartz	17
As	0.354	Calcite	14
Ba	0.025	Dolomite	2
Bi	0.010	Muscovite	2
Ca	3.96	Chlorite	5
Cd	0.011	**Pyrite**	**54**
Co	0.033	**Sphalerite**	**1**
Cu	0.100	**Galena**	**1**
Fe	41.8	**Pyrrhotite**	**4**
Mg	0.556		
Mn	0.163		
Pb	1.06		
S	31.1		
Sb	0.022		
Ti	0.033		
Zn	0.977		

The tailings porewater and the process water were sampled and analysed for pH and Eh (redox potential) using the electrode method, , electrical conductivity (EC) using a conductivity meter, and metals and total sulfur using ICP-AES. Table 3 contains the chemical composition of the tailings porewater and process water. Pore and process waters have close chemical compositions. The high sulfate content (4,588 and 4,528 mg/L for pore and process waters, respectively) could have a strong influence on the cement hydration process and thus on compressive strength development. The hydration process could also be affected by the relatively high amounts of zinc (0.668 and 0.258 mg/L for pore and process waters, respectively) and lead (0.526 and 0.993 mg/L for pore and process waters, respectively).

Table 3 Geochemistry and chemical compositions of the BWK mine tailings pore and process waters

Parameter	Unit	Detection limit	Porewater	Process water
pH			8.0	7.3
Eh	mV		70	15.2
EC	µS		11,920	12,470
Al	mg/L	0.010	<0.01	0.072
Ba	mg/L	0.001	0.045	0.044
Co	mg/L	0.004	0.006	<0.004
Cu	mg/L	0.003	0.135	2.33
Fe	mg/L	0.006	0.035	0.034
Mg	mg/L	0.001	31.5	5.55
Mn	mg/L	0.002	0.133	0.066
Mo	mg/L	0.009	0.043	0.026
Ni	mg/L	0.004	0.007	0.005
Pb	**mg/L**	0.020	**0.526**	**0.993**
S_{tot}	mg/L	0.090	1,880	3,870
SO_4^{2-}	**mg/L**	1	**4,588**	**4,528**
Sb	mg/L	0.090	0.208	0.605
Si	mg/L	0.020	3.32	0.615
Zn	**mg/L**	0.005	**0.668**	**0.258**

2.2 Cemented paste backfill mixtures preparation and curing conditions

CPB mixtures were prepared by mixing the three ingredients (tailings, binder and water) using a Hobart electric mixer (model D 300-1) for 5 to 7 minutes. The binding agent used was the high sulfate-resistant Portland cement type HS (formerly type V or 50). Five different CPB mixtures were prepared with five mass concentrations of cement (C_b), being 0, 1, 1.5, 1.75 and 2 wt%. Each paste mixture was prepared with the following characteristics: solid mass concentration (%C_w) fixed at 83% (corresponding slump between 140 and 165 mm. It should be noted that the high value of C_w is directly related to the value of G_s, which is around 4. Mixing water was the BWK mine process water. The consistency of the paste was determined by the ASTM C143/C143M-20 Standard slump test using the 300 mm Abrams cone. Once prepared, the CPBs were cast in 76 mm diameter and 152 mm high capped plastic moulds and then cured in a humid room at a temperature of 25°C ± 2°C with >90% relative humidity for three curing times (3, 7 and 28 days). In BWK mine practices, the mass concentration of cement (C_b) and its relation to the cement mass ratio ($\%B_w$) are given by the following equations:

$$C_b\ (\%) = 100 \times M_{\text{cement}} \big/ \left(M_{\text{cement}} + M_{\text{dry\_tailings}} + M_{\text{water}} \right) = 100 \times \left(M_{\text{cement}} / M_{\text{CPB}} \right) \tag{1}$$

$$\%B_w = 100 \times \left(M_{\text{cement}} / M_{\text{dry\_tailings}} \right) = 100 \times M_{\text{cement}} \big/ \left(M_{\text{CPB}} - M_{\text{cement}} - M_{\text{water}} \right) \tag{2}$$

$$C_b(\%) = \%C_{\text{w}} \cdot \%B_{\text{w}} \big/ \left(100 + \%B_{\text{w}} \right) \quad \text{and} \quad \%B_{\text{w}} = 100 \cdot C_b(\%) \big/ \left[\%C_{\text{w}} - C_b(\%) \right] \tag{3}$$

where:

$\%B_w$ = percent cement-to-dry tailings ratio (wt%).

M_{cement} = mass of cement added (kg, tonne).

$M_{\text{dry\_tailings}}$ = mass of dry tailings in the mixture (kg, tonne).

M_{water} = total mass of water (kg, tonne).

M_{CPB} = mass of cemented paste backfill prepared (kg, tonne).

$\%C_w$ = $100 \times (M_{\text{dry\_tailings}} + M_{\text{cement}})/M_{\text{CPB}}$ = solid mass concentration in CPB (wt%).

The average index parameters of the fresh BWK mine CPB (degree of saturation S_r = 1.0) are:

wet density ρ_{wet} = 2.62 g.cm^{-3}.

wet unit weight γ_{wet} = 26 kN.m^{-3}.

dry density ρ_d = 2.20 g.cm^{-3}.

dry unit weight γ_d = 21.6 kN.m^{-3}.

initial void ratio e_0 = 0.80.

initial porosity n_0 = 45%.

The corresponding volumetric solids concentration C_v (v/v%) = $\%C_w \rho_{wet}/\rho_s$ is given in Table 4 and summarises the CPB batch mixing parameters (C_b, B_w, C_w, W/C, C_v and slump height S).

Table 4 CPB batch mixing parameters

#Batch	Cement content C_b (wt%)	Cement ratio B_w (wt%)	Water-to-cement ratio W/C	Solids mass concentration C_w (wt%)	Volume solids concentration C_v (v/v%)	Slump S	
						(mm)	(inch)
B1	0	0	0	83.3	55.3	158	6.22
B2	1	1.22	17.0	83.4	59.0	158	6.22
B3	1.5	1.84	11.3	82.9	58.7	155	6.10
B4	1.75	2.15	9.7	83.1	59.2	146	5.75
B5	2	2.47	8.5	82.9	59.1	155	6.10

2.3 Testing program

2.3.1 Unconfined compression tests

After each curing time (3, 7 and 28 days), CPB specimens were subjected to uniaxial compression tests performed using an MTS 10/GL hydraulic press having a maximum capacity of 50 kN and run at a constant displacement rate of 1 mm/min according to ASTM C39/C39M-21 Standard. The tests were carried out in triplicate and a data acquisition system recorded the axial strain and the normal stress applied to the specimens during the test. From these data, the peak (ultimate) value corresponds to the UCS. Note that each UCS value after each curing time is obtained by averaging three values (triplicate). The gravimetric water content of broken specimens was also determined.

2.3.2 Undrained triaxial compression tests

Three CPB mix formulations (based on the mass concentration of cement, C_b%) were selected for the CIU and porewater pressure measurement (CIU+u) tests: C_b = 1.5 wt%, 1.75 wt% and 2 wt%. The specimens with 1 wt% cement were too soft to be placed in the triaxial cell. The three low cement contents were selected to evaluate the undrained shear strength as well as the intrinsic parameters (effective cohesion c' and angle of friction ϕ') of CPBs at early ages (3 and 7 days). The tests were performed according to ASTM D4767-11 and using a GDS Triaxial Automated System (TAS) as shown in Figure 2.

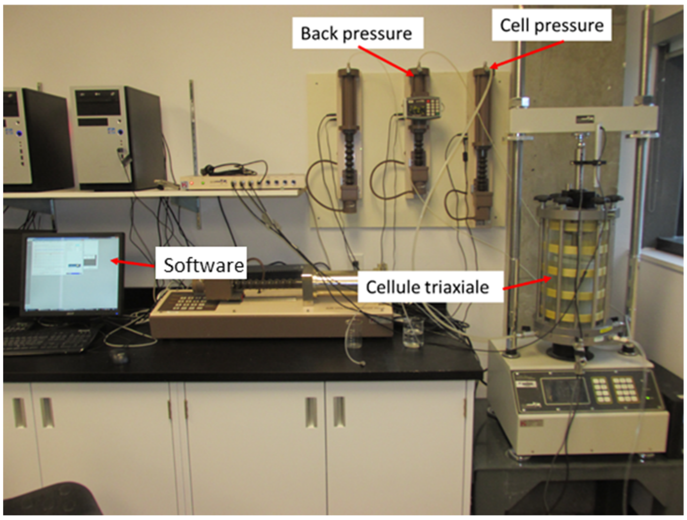

Figure 2 General set-up of the GDS TAS used

Keeping in mind the importance of better controlling the pressure on the barricade during continuous filling, assuming an at-rest coefficient of earth pressure K_0 = 0.5 (ϕ' = 30°), and considering a height equivalent to the height of the backfill plug (h = 7 m), the calculated total horizontal stress σ_{h0} (equivalent to triaxial cell or confining pressure, σ_c or σ_3) is 125 kPa ($\sigma_{h0} = \sigma'_{h0} + u_0$). Indeed, the calculations give vertical effective stress σ'_{v0} = 113 kPa and horizontal effective stress σ'_{h0} = 57 kPa (γ_{wet} = 26 kN/m^3, γ' = 16.2 kPa/m, $u_0 = \gamma_w h_w$ = 69 kPa). Therefore, the selected confining pressure σ_3 was selected in the range 5–100 kPa, depending on the C_b% and curing time. Table 5 presents the three different confining pressures (σ_3) used for testing each mixture recipe.

Table 5 Confining pressures selected for the undrained triaxial compression tests

Test no.	Applied cell pressure (σ_c) or confining pressure σ_3 (kPa)					
	1.5% cement Curing time (days)		1.75% cement Curing time (days)		2% cement Curing time (days)	
	3-day	7-day	3-day	7-day	3-day	7-day
#1	5	15	10	20	15	25
#2	10	30	20	40	30	50
#3	20	60	40	80	60	100

2.3.3 Assessment of the static liquefaction of CPB at early ages

The susceptibility to static liquefaction of CPB at early ages was evaluated through conventional triaxial compression testing (CIU+u). The specimens are placed into a triaxial cell and a confining pressure is applied for isotropic consolidation. Undrained triaxial tests are then performed after 3 and 7 days of curing. The undrained condition was selected because static or dynamic liquefaction occurs only under undrained conditions where the potential of excess pore pressure (u_e) development or large plastic deformation is highest. Static liquefaction can be triggered under monotonic loading such as during the CIU+u triaxial tests. The conditions for static liquefaction triggering are either null effective minor stress ($\sigma'_3 = 0$) or when the pore pressure ratio r_u (= $\Delta u_e/\sigma'_3$) reaches unity ($r_u = 1$). This is possible only if the CPB exhibits contractive behaviour.

3 Results and discussion

3.1 Unconfined compressive strength

Table 6 presents the results of the unconfined compression tests performed at 3, 7 and 28 days of curing. These results indicate that a minimum of 1.5 wt% of cement is required to develop a UCS >50 kPa after 7 days of curing. Indeed, with only 1 wt% of cement, UCS remains below 100 kPa even after 28 days of curing. A cement content of 1.5 wt% allows the development of a UCS >150 kPa after 28 days of curing. Nevertheless, at a young age of 3 days, the UCS remains lower than 100 kPa. Moderately high UCS values were obtained with 1.75 wt% and 2 wt% of cement. Data in Table 6 can be mainly used to determine how the BWK mine CPB cement content can be lowered while maintaining the same strength performance. It is recommended, however, to consider only the 28 days curing data due to the high variability of the UCS values between 3 and 7 days of curing.

Table 6 BWK mine CPB UCS values after 3, 7 and 28 days of curing time

#Batch	Cement content C_b (wt%)	Binder ratio B_w (wt%)	3 days		7 days		28 days	
			UCS (kPa)	w (wt%)	UCS (kPa)	w (wt%)	UCS (kPa)	w (wt%)
B1	0	0	0	16.9	0	17.0	0	17.1
B2	1	1.2	15	18.8	25	18.7	40	18.5
B3	1.5	1.8	23	19.4	66	19.1	163	18.5
B4	1.75	2.2	51	18.7	162	18.6	268	18.5
B5	2	2.5	69	19.4	218	18.7	405	18.1

3.2 CIU+u triaxial compression test results

3.2.1 Undrained shear properties of CPB at early ages

Figures 3 and 4 present the curves of shear stress ($q = [\sigma'_1 - \sigma'_3]/2$) and excess porewater pressure (u_e) as a function of axial strain ($\varepsilon_a = \Delta H/H_0$) of the backfill samples after 3 days and 7 days of curing, respectively. Overall it can be observed that after 3 days of curing time (Figure 3) the CPB exhibits an elastic-plastic mechanical behaviour with a strain hardening, while after 7 days of curing time this strain hardening behaviour disappears and the behaviour is only elastic-plastic or strain softening. This is shown by the appearance of a plateau after the peak at about 5% axial strain (Figure 4).

Regarding the pore pressure curves as a function of the axial deformation, it is observed that from an axial deformation >4.5% the pore pressure becomes negative (change of the internal structural of the CPB).

Figure 5 presents the stress paths for the tests performed. A stress path represents the relation between the shear stress $q = [\sigma'_1 - \sigma'_3]/2$) and mean effective normal stress p' (= $[\sigma'_1 + \sigma'_3]/2$).

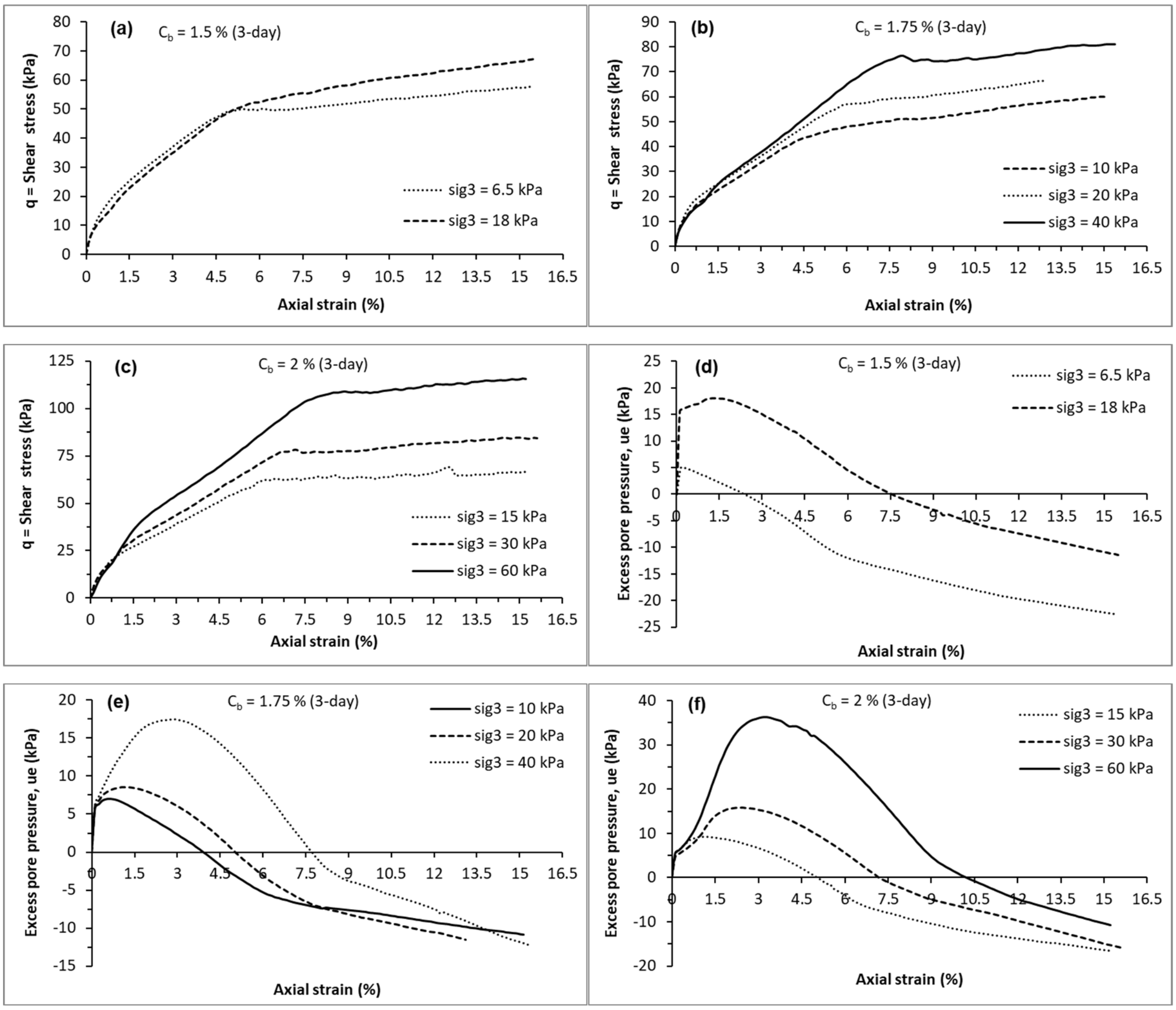

Figure 3 Undrained shear test results after 3 days of curing: (a), (b), (c) Shear stress versus axial strain for C_b = 1.5, 1.75 and 2 wt%, respectively; (d), (e), (f) Excess porewater pressure versus axial strain for C_b = 1.5, 1.75 and 2 wt%, respectively

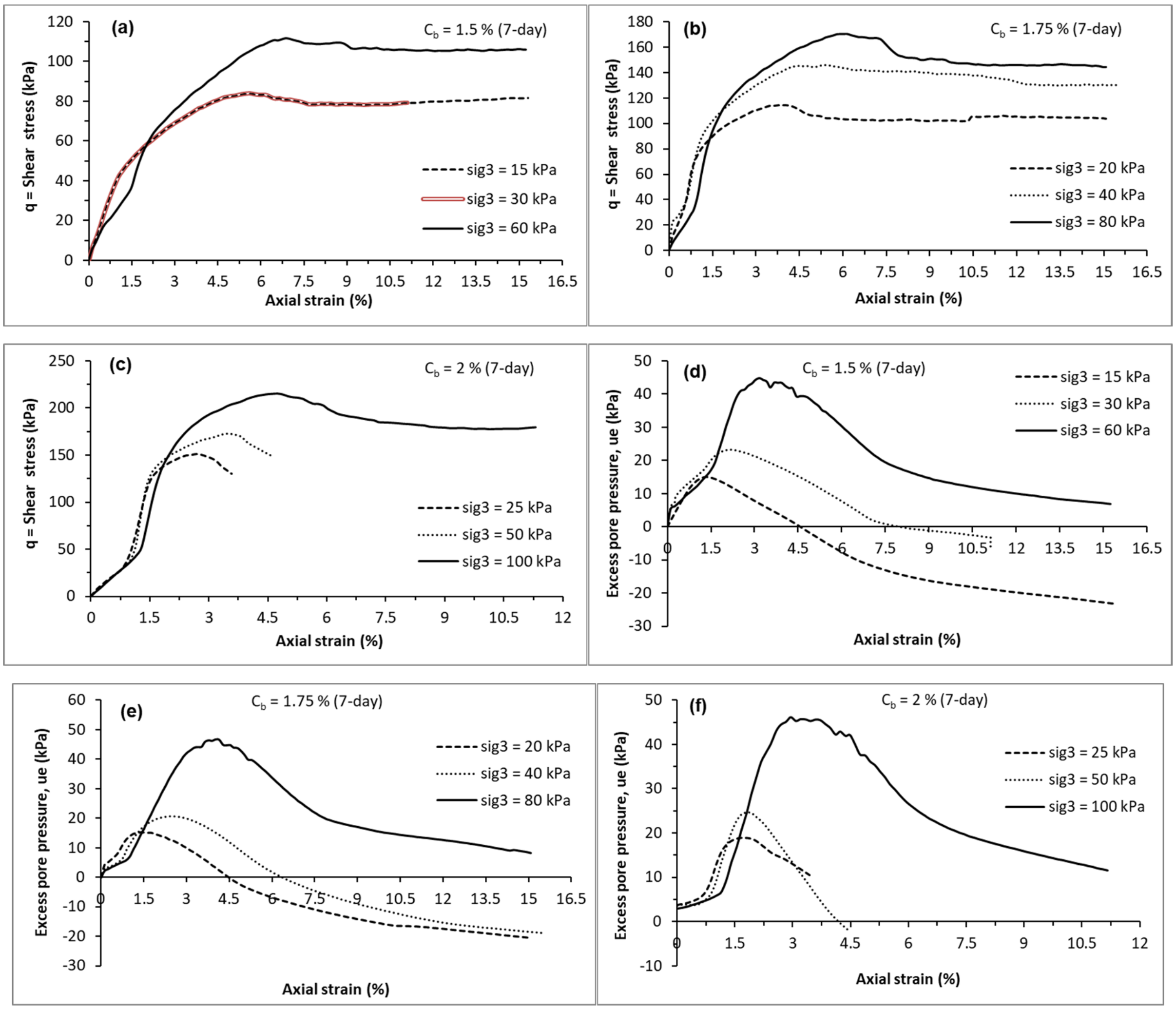

Figure 4 Undrained shear test results after seven days of curing: (a), (b), (c) Shear stress versus axial strain for C_b = 1.5, 1.75 and 2 wt%, respectively; (d), (e), (f) Excess porewater pressure versus axial strain for C_b = 1.5, 1.75 and 2 wt%, respectively

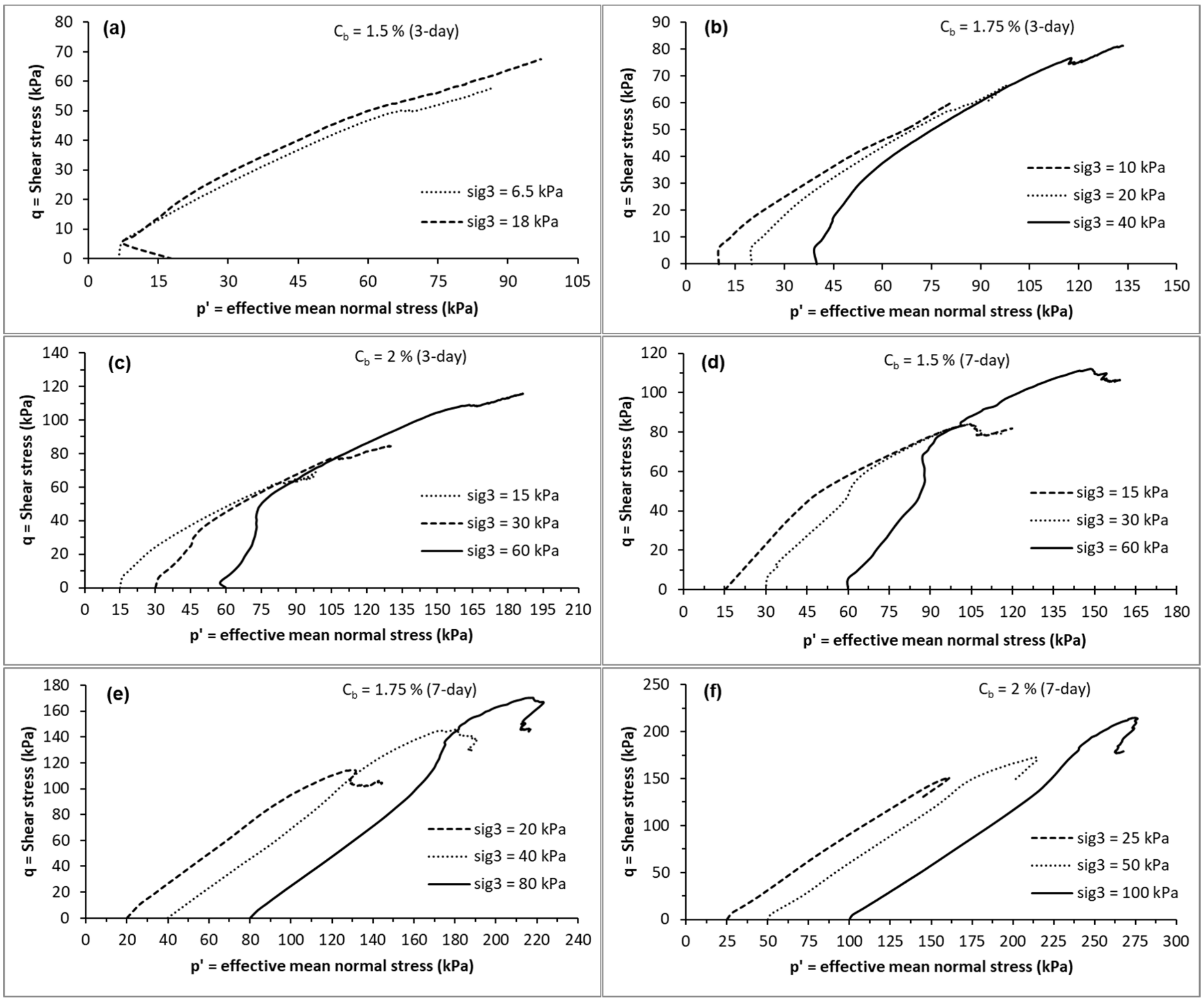

Figure 5 Stress path during the undrained shear tests: (a), (b), (c) After a 3-day curing time for C_b = 1.5, 1.75 and 2 wt%, respectively; (d), (e), (f) After 7-day curing time for C_b = 1.5, 1.75 and 2 wt%, respectively

3.2.2 Intrinsic parameters of the CPB mixtures at early ages

The triaxial CIU+u test results can be used for determining Mohr–Coulomb intrinsic parameters *c'* (effective cohesion) and *ϕ'* (effective angle of friction). These parameters are derived from the plots of the mean effective stress *p'* (= $[\sigma'_1+\sigma'_3]/2$) and the peak shear stress *q* ($[\sigma'_1-\sigma'_3]/2$) as shown in Figure 6. Table 7 contains the calculated values of *p'* and *q* (MIT stress path analysis method) for all triaxial tests except for the test on CPB with C_b = 1.5 wt% cement and cured at 3 days. This test failed because the sample was deformed and no peak was observed.

Table 7 Mean effective stress p' and shear stress q (in kPa)

	C_b = 1.5% (7-d)		C_b = 1.75% (3-d)		C_b = 1.75% (7-d)		C_b = 2% (3-d)		C_b = 2% (7-d)	
	p'	*q*	*p'*	*q*	*p'*	*q*	*p'*	*q*	*p'*	*q*
	(kPa)		(kPa)		(kPa)		(kPa)		(kPa)	
Test #1	102	84	56	44	131	114	82	62	161	151
Test #2	104	84	78	56	173	145	108	78	213	173
Test #3	148	112	118	77	218	170	161	109	275	215

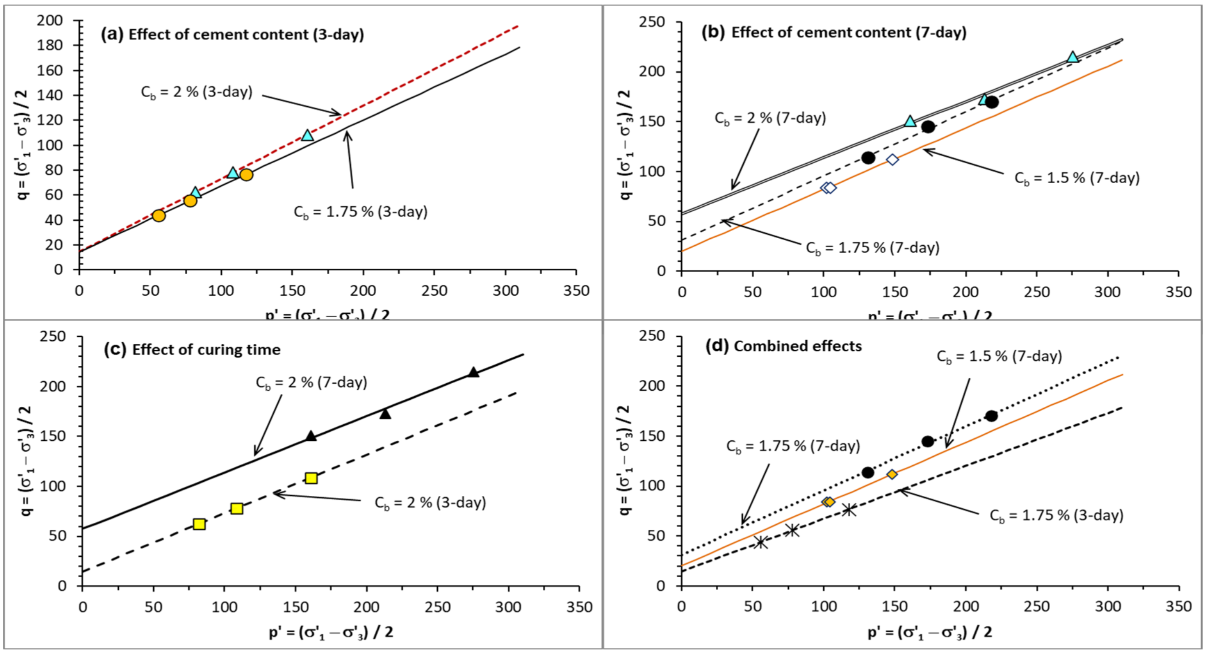

Figure 6 Mohr–Coulomb failure criterion: (a), (b) Effect of the cement content after 3 and 7 days of curing; (c) Effect of curing time; (d) Combined effects of curing time and cement content

In Figure 6, each straight line is described by a linear equation of the form:

$$q = p' \times \tan\alpha' + a' \quad \text{or} \quad \frac{\sigma'_1 - \sigma'_3}{2} = a' + \frac{(\sigma'_1 + \sigma'_3)}{2}\tan\alpha' \tag{4}$$

From the slope tan (α′) and intercept *a′*, the Mohr–Coulomb parameters *c′* and ϕ' can derived as follows:

$$\phi' = \sin^{-1}(\tan\alpha') \qquad \text{and} \qquad c' = \frac{a'}{\cos\phi'} \tag{5}$$

From Figure 6 and Equation 5 the effective cohesion (*c′*) and angle of internal friction (ϕ′) are calculated and presented in Table 8. One interesting observation is that the effective angle of friction ϕ′ is almost constant regardless of the cement content (C_b) and the curing time (*t*). This agrees with Thompson et al. (2012) but with a lower friction angle (ϕ′ = 37°). This is an indication that tailings will define the friction angle. In contrast, the effective cohesion (*c′*) varies regarding cement content and curing time.

Table 8 Intrinsic parameters of the BWK mine CPB at early ages

	C_b = 1.5 wt%	C_b = 1.75 wt%		C_b = 2 wt%	
	7-day	3-day	7-day	3-day	7-day
ϕ'(deg)	32	28	33	30	29
c' (kPa)	24	16	37	17	66
K_0 (= 1- sinϕ')	0.47	0.53	0.46	0.49	0.51

3.3 Susceptibility of CPB to static liquefaction

Figures 7 and 8 present the different curves allowing to evaluate the susceptibility of CPBs to static liquefaction following a type of rapid loading and under undrained conditions. Static liquefaction is triggered under monotonic loading such as during the CIU+u triaxial tests.

The conditions for static liquefaction triggering are either null effective minor stress ($\sigma'_3 = 0$) or when the pore pressure ratio r_u ($= \Delta u/\sigma'_3$) reaches unity ($r_u = 1$). These two conditions can only be verified (or met) if the fresh cemented paste backfill exhibits contractive behaviour.

All results in Figures 6 and 7 show that the CPB contracts at the beginning of loading (maximum axial strain in the range 0.5–~3.5%) before exhibiting a dilative behaviour for the largest deformations. The contractive nature of the CPB leads to the development of excess pore pressure (susceptibility to static liquefaction) while the dilative nature of the CPB leads to the decrease of pore pressure (no static liquefaction).

These figures confirm the occurrence of static liquefaction only with the CPB mixes prepared with 1.5% cement after 3 days of curing (Figures 7a and d) and 7 days of curing (Figures 8a and d), and with the lowest confining pressures (σ_3 = 15 and 18 kPa).

This initial static liquefaction occurred from the onset of undrained shear to an axial strain of about 1.5% (reached after about six minutes of shear).

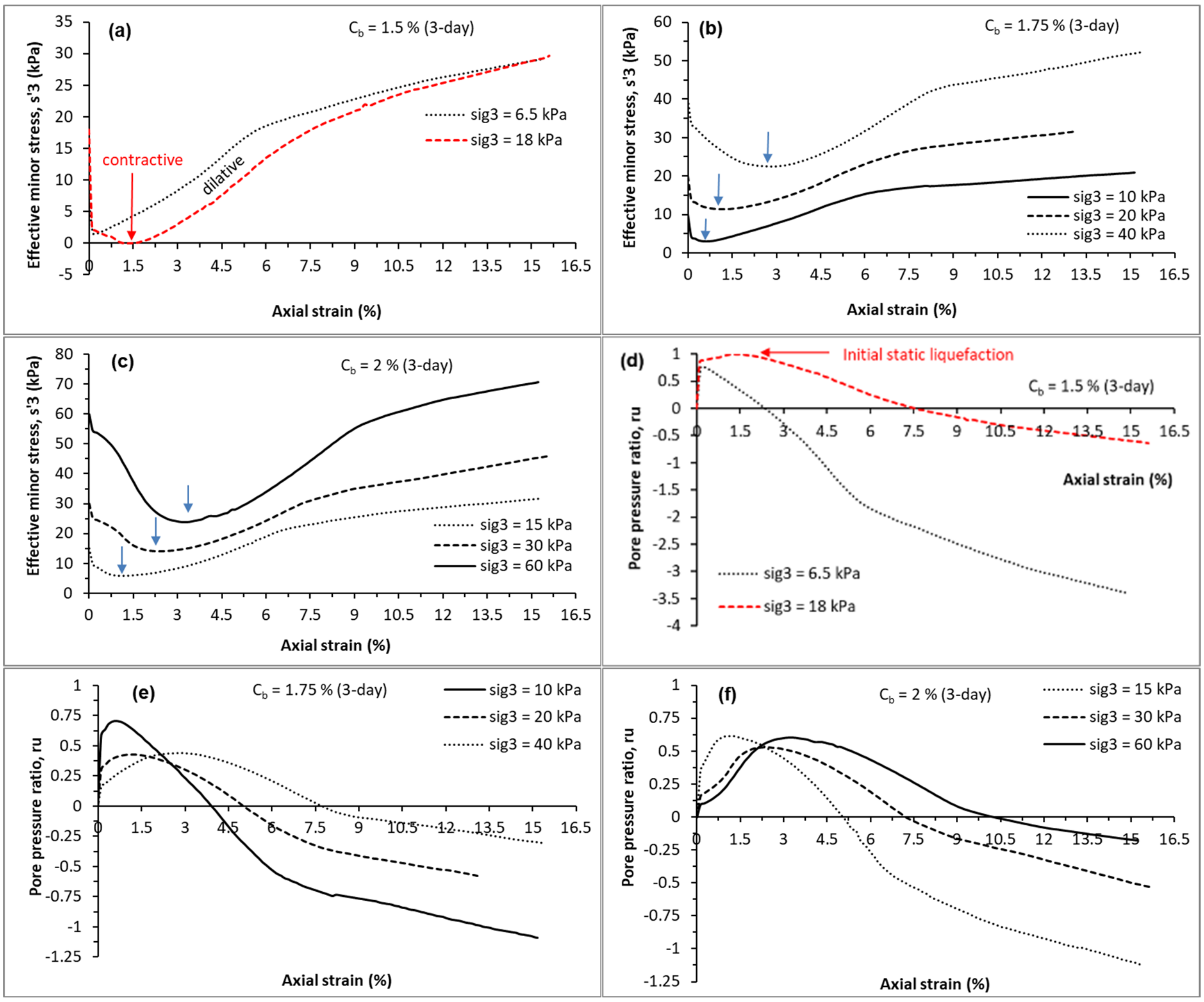

Figure 7 Evaluation of the susceptibility of CPB to static liquefaction after a 3-day curing time: (a), (b), (c) Evolution of σ'_3 versus axial strain curves for C_b = 1.5, 1.75 and 2 wt%, respectively; (d), (e), (f) Evolution of pore pressure ratio (r_u) versus axial strain curves for C_b = 1.5, 1.75 and 2 wt%, respectively

Furthermore, knowing the values of σ_1 (when σ'_3 = 0), the equivalent heights of the backfill (h_{eq}) can be calculated as follows:

$$h_{eq} = \sigma_1 / \gamma_{wet} \tag{6}$$

where:

γ_{wet} = wet unit weight of the fresh CPB (kN.m^{-3} or kPa.m^{-1}).

Considering the average wet unit weight γ_{wet} = 26 kPa/m, Equation 6 gives an equivalent fill height (h_{eq}) varying between 2.4 m (for the 3-day cured specimens) and 4.2 m (for the 7-day cured specimens). Therefore, it can be stated that for CPB (at least, for the case of the BWK mine CPB studied), the appearance of static liquefaction during rapid static loading under undrained conditions would only be temporary and of short duration (ε_a = 1.5%, duration varying between 327 and 360 seconds, respectively, for the 3-day and 7-day cured specimens). Indeed, all the tests showed that the backfill contracted then dilated for large deformations (zero susceptibility to static liquefaction).

In the practice of underground mine backfilling, it is improbable that a backfill stope will have one of its faces exposed after a backfill height of only between 2.4 and 4.2 m. Therefore, static liquefaction would not appear to be a major operational risk that could result in equipment damage or unplanned shutdowns. Similar observations were made in the pioneering study by Aref (1988). Future work should look at the strength at less than 3 days to investigate the characteristics of the backfill under those conditions. The authors are not sure if it is relevant with these mixtures, as the mass concentration of cement [C_b(%)] is so low and UCS is extremely low at 3 days.

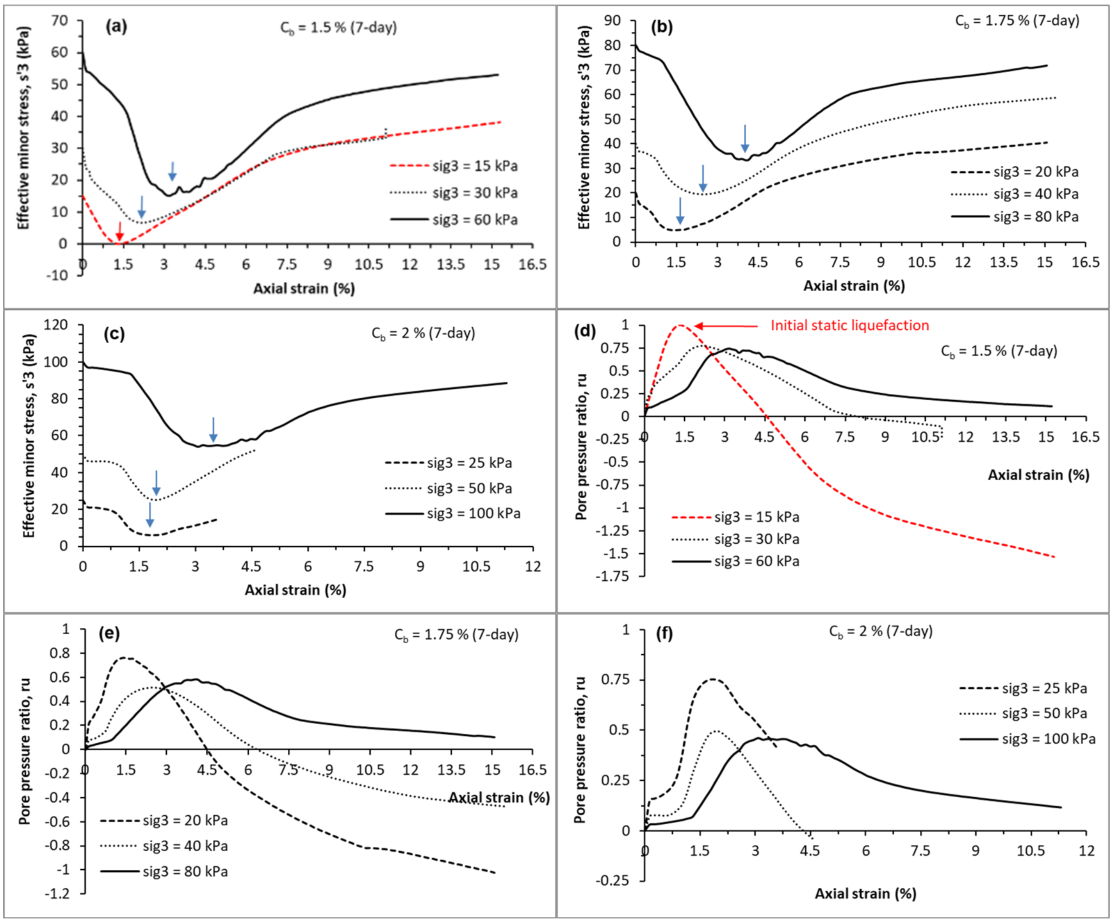

Figure 8 Evaluation of the susceptibility of CPB to static liquefaction after a 7-day curing time: (a), (b), (c) Evolution of σ'_3 versus axial strain curves for C_b = 1.5, 1.75 and 2 wt%, respectively; (d), (e), (f) Evolution of pore pressure ratio (r_u) versus axial strain curves for C_b = 1.5, 1.75 and 2 wt%, respectively

4 Conclusion

The main purpose of this study was to assess the susceptibility of the early age CPB (between 3 and 7 days) to static liquefaction from an operational risk analysis perspective related to the underground backfilling process. An experimental study was carried out for this purpose and made it possible to characterise the undrained shear strength (CIU tests) of different formulations of weakly CPB mixtures (with cement mass content ≤ 2 wt%).

- The results of this experimental investigation showed that for the three cement contents C_b (1.5, 1.75 and 2 wt%) and at the two curing times (3 and 7 days) tested, only CPB mixes with C_b = 1.5 wt% cement verified (or met) the condition of initial static liquefaction temporarily before resisting liquefaction development (dilative behaviour).
- It can be concluded that the occurrence of static liquefaction during rapid static loading of cemented paste backfill would only be temporary and of short duration (< 10 minutes). Therefore, static liquefaction would not appear to be a major operational risk that could result in the disruption of underground mining operations.
- The results of 7-day curing with 1.5% binder had a UCS of 66 kPa, and testing showed signs of potential liquefaction at low confinement (σ_3 = 15 kPa). le Roux et al. (2004) found that a UCS of 37 kPa after 12 hours of curing time could resist dynamic liquefaction. This is why instrumentation and laboratory testing are required to understand the material for each different mining project. This would be important to understanding the potential loading conditions on the barricades.

Acknowledgement

The authors would like to thank their university, Université du Québec en Abitibi-Témiscamingue, and the Government of Canada for their financial support through the Research and Creation Grants – Support for the realisation of short projects (#FIRC/FUQAT 2021-2022), and the NSERC Discovery Grant (#RGPIN-2019-04946), respectively. The authors would also like to acknowledge AEM Ltd for its partnership and financial support through the Research Institute of Mines and Environment.

References

Aref, K 1988, *A Study of the Geotechnical Characteristics and Liquefaction Potential of Paste Backfill*, PhD thesis, McGill University, Montreal, 620 p.

ASTM International 2020, *Standard Test Method for Slump of Hydraulic-Cement Concrete (ASTM C143/C143M-20)*, ASTM International, West Conshohoken.

ASTM International 2020, *Standard Test Method for Consolidated Undrained Triaxial Compression Test for Cohesive Soils (ASTM D4767-11)*, ASTM International, West Conshohoken.

ASTM International 2021, *Standard Test Method for Compressive Strength of Cylindrical Concrete Specimens (ASTM C39/C39M-21)*, ASTM International, West Conshohoken.

Aubertin, M, Bussière, B, Bernier, L, Chapuis, R, Julien, M, Belem, T & Li, L 2002, 'La gestion des rejets miniers dans un contexte de développement durable et de protection de l'environnement', *Comptes-rendus du Congrès Annuel de la Société Canadienne de Génie Civil*.

Belem, T, Effenguet, H & Mbonimpa M 2013, 'Estimation of required minimum binder content by assessing the liquefaction potential of early age cemented mine backfill', *Proceedings of the 66th Canadian Geotechnical Conference*, The Canadian Geotechnical Society, Vancouver.

Belem, T & Benzaazoua, M 2008, 'Underground mine paste backfill technology: applications and design methods,' *Geotechnical and Geological Engineering*, vol. 26, no. 2, pp. 147–174.

Belem, T & Mbonimpa, M 2016, 'Minimum strength required for resisting to cyclic softening/failure of cemented paste backfill at early age', *Proceedings of the 3rd International Symposium on Mine Safety Science and Engineering*, McGill University, Montreal.

Belem, T, Benzaazoua, M & Bussière, B 2000, 'Mechanical behaviour of cemented paste backfill', *Proceedings of the 53rd Annual Conference of the Canadian Geotechnical Society*.

Benzaazoua, M, Belem, T & Bussière, B 2002, 'Chemical aspect of sulfurous paste backfill mixtures', *Cement and Concrete*, vol. 32, no. 7, pp. 1133–1144.

Benzaazoua, M, Fall, M & Belem, T 2004, 'A contribution to understanding the hardening process of cemented pastefill', *Minerals Engineering*, vol. 17, no. 2, pp. 141–152.

Davies, M, McRoberts, E, & Martin, T 2002, 'Static liquefaction of tailings – fundamentals and case histories', *Proceedings of Tailings Dams 2002*.

Fourie, AB, Blight, GE & Papageorgiou, G 2001, 'Static liquefaction as a possible explanation for the Merriespruit tailings dam failure', *Canadian Journal Geotechnical Journal*, vol, 38, pp. 707–719.

Grice, T 1998, 'Underground mining with backfill', *Proceedings of the 2nd Annual Summit on Mine Tailings Disposal Systems*.

Kramer, SL & Seed, HB 1988, 'Initiation of soil liquefaction under static loading conditions', *ASCE Journal of Geotechnical Engineering*, vol. 114, no. 4, pp. 412–430.

le Roux, K, Bawden, W & Grabinsky, M 2004, 'Liquefaction analysis of early age cemented paste backfill', *Proceedings of The Eighth International Symposia on Mining with Backfill*, pp. 233–241.

Potvin, Y, Thomas, E & Fourie, AB (eds) 2004, *Handbook on Mine Fill*, Australian Centre for Geomechanics, Perth.

Poulos, SJ, Castro, G & France, JW 1985, 'Liquefaction evaluation procedure', *ASCE Journal or the Geotechnical Engineering*, vol. III, no. GT6, pp. 772–792.

Sladen, JA, D'Hollander, RD & Krahn, J 1985, 'The liquefaction of sands, a collapse surface approach', *Canadian Geotechnical Journal*, vol. 22, no. 4, pp. 564–578.

Thompson, BD, Bawden, WF & Grabinsky, MW 2012, 'In situ measurements of cemented paste backfill at the Cayeli Mine', *Canadian Geotechnical Journal*, vol. 49, no. 7, pp. 755–772.